Hindawi
Shock and Vibration
Volume 2021, Article ID 5586177, 9 pages
https://doi.org/10.1155/2021/5586177

Research Article

Transition Effect on the Flow Dynamics in a Compressor Blade Passage

Ryszard Szwaba, Piotr Kaczynski, and Janusz Telega

Institute of Fluid-Flow Machinery, Polish Academy of Sciences (IMP PAN), Fiszera 14, 80–952, Gdansk, Poland

Correspondence should be addressed to Ryszard Szwaba; ryszard.szwaba@imp.gda.pl

Received 26 January 2021; Revised 22 March 2021; Accepted 20 April 2021; Published 28 April 2021

Academic Editor: Athanasios Chasalevris

An experimental investigation was carried out to study the effect of the boundary layer transition on the flow dynamics in the blade passage of a compressor cascade. A model of a turbine compressor passage was designed and assembled in a transonic wind tunnel for this purpose. Two different flow control methods were used in the experiment to induce the transition upstream of the shock wave, one concerning the microstep application and the other using distributed roughness strips. Two locations of spanwise microsteps for the transition trigger were chosen, one at the leading edge and the other closer to the shock wave position. The distributed roughness in the form of standard sandpaper strips with different heights was applied in three various locations on the blade upstream of the shock. The main objective of investigations is to present the influence of the laminar and turbulent shock wave-boundary layer interaction on the flow dynamics in a compressor fan passage, and the specific objective is to show how the parameters of particular transition control methods affect the flow dynamics in the investigated channel. The major challenge for this research was to minimize the disturbance caused by the microstep or roughness to the laminar boundary layer, while still ensuring a successful transition. Very interesting results were obtained in the flow control application for the boundary layer transition control, demonstrating a positive effect on the flow unsteadiness in changing the nature of the interaction.

1. Introduction

The compressor and turbine efficiency of an airplane engine depend to a great extent on the state of the boundary layers developing along the surfaces of these parts. A large part of the drag or losses in aerodynamic devices in the flow is related to skin friction; decreasing the friction will significantly contribute to their reduction. One of the available solutions to achieve lower drag friction is to extend the laminar flow on the overflow surface. Therefore, intensive research concerning the laminar flow is carried out nowadays [1–3]. In the case of a civil turbofan engine operating at particularly high altitudes (for jets even 15 km), the Reynolds number can drop by a factor of 4 in comparison to the sea level values. The laminar boundary layer on the transonic compressor rotor blades will interact with shock waves, and a strong boundary layer separation will appear as a result. This can seriously affect the aero-engine performance and operation. One way to avoid strong separation is to control the boundary layer transition to the turbulent state upstream of the shock wave location. Transition within the boundary layer can be forced through application of surface roughness [4], a turbulator step [5], or air-jet vortex generators (AJVG) [6]. Although such passive control methods are already in use for the boundary layer separation control [7, 8], the mechanism of the shock wave-laminar boundary layer interaction and, in particular, the source of the strong shock unsteadiness are still not well understood. Such strong shock unsteadiness through pressure pulsations, partially driven by a separated boundary layer, often leads to unsteady loading of blades. Such unsteady loading of blades is not acceptable, and shock wave interaction with the laminar boundary layer should be avoided, especially when such interaction becomes strongly unsteady and causes vibrations of blades [9] which can be also propagated on the whole turbofan rotor.

In a long term, unsteady aerodynamic loads for the structure lead to the fatigue of the material [10, 11]. The sources of such unsteadiness come from the compressibility effects at high speed, and they are sources of flow-induced vibrations, crucial for the stability of components. By application of flow control methods for suppressing the boundary layer separation, the knowledge of the effects of their action is gained and appropriate control methods in respect of mitigation of unsteadiness may be suggested. The introduction of extensive regions of a laminar flow in blade passages demands a careful flow control approach to avoid laminar interactions with a shock wave. This means that the transition to turbulence should take place upstream of the interaction. However, when the transition is provoked too far upstream, a large part of the beneficial laminar flow region is lost. The main challenge is to gain knowledge of where the transition should be induced with respect to the mitigation of unsteadiness. This knowledge will enable the implementation of an effective laminar flow technology for engines in which the interaction of a laminar boundary layer with a shock wave also takes place and causes severe problems. Primarily, the first rotor disk of a compressor has such a large diameter that transonic velocities at the blade tip are achieved. In combination with the low density under cruise conditions, the Reynolds number is reduced so much that the extent of the laminar boundary layer along the cord may reach the shock wave and a strong separation may be induced as a consequence. In some conditions of the compressor operation (especially at a high altitude in cruise conditions), this separation leads to strong unsteady effects [12, 13] and may provoke the compressor surge and blade vibrations, reducing the propulsion system performance considerably.

The main objective of the paper is to present an experimental investigation concerning the influence of the laminar and turbulent shock wave-boundary layer interaction on the flow dynamics, i.e., on unsteadiness in a compressor fan passage. It is well known that flow separation is at the origin of low-frequency flow fluctuations. In a supersonic internal channel flow, such unsteadiness affects the whole interaction including the shock system [14]. Therefore, measurements of the shock oscillation can be used to estimate the channel flow in the aspect of its nonstationary characteristics, and hence, the flow unsteadiness in the blade passage was determined by means of measurements of shock oscillations. Shock oscillations, especially at low frequencies and with a high amplitude, originate from pressure pulsations in the separation zone [15] and reflect pressure fluctuations in the channel space in a more holistic way. A pressure transducer measures this value on a very local scale only.

Flow control with a shock wave is usually introduced in the context of reduction in losses [16] in this flow, and the influence of the applied control method on the reduction of the unsteady effects is usually of secondary importance. Therefore, the article presents the influence of different control methods and the location on the unsteady effects in the flow. It is proposed to use a tripping device, a microstep, and distributed roughness to generate the boundary layer transition upstream of the shock for the transition control. Different roughness locations and its size were tested to check whether the induced transition upstream of the shock could improve the pressure unsteadiness, and hence the structure vibrations.

The major challenge for this research was to minimize the disturbance caused by the microstep or roughness to the laminar boundary layer, while still ensuring a successful transition. Few flow cases concerning the roughness application effect on the shock wave-boundary layer interaction can be found in the literature. They concern mainly the basic research with an oblique shock wave (in this case, the interaction is weaker in comparison to a normal shock wave) in convergent-divergent nozzles [17, 18]. Hence, as flow control devices in a laminar boundary layer are very poorly represented in the subject literature, one of the most important issues was to use the roughness size, above which negative effects of its application can be observed, i.e., overtripping of the boundary layer and further growth of the flow unsteadiness.

2. Experimental Setup

The research presented in this paper was a part of the EU TFAST project which was focused on transition and its location effect on the shock wave-boundary layer interaction (SWBLI). The topic of the laminar/transitional/turbulent interaction with a shock wave is a most challenging problem in aeronautics, even more, when unsteady interaction effects play a crucial role, and the goal of the flow control application is to make this interaction with minimum adverse effects (such as separation and unsteadiness). Different tripping devices may be used to induce the transition in the boundary layer; however, the presented experiments focused on the effects of roughness and microsteps on the unsteady aerodynamic phenomena in a compressor fan blade passage. For this purpose, a model of a compressor passage was designed and assembled in a wind tunnel [19] (at the Institute in Gdansk) in order to investigate the flow structure on the suction side of the blade. The compressor passage model was mounted in a rectilinear test section of a transonic wind tunnel, as shown in Figure 1(a). The model in the region marked by the dashed curve in Figure 1(b) can reproduce the interblade flow structure similar to the one as on the profile in the reference cascade [20]. It produces a proper shock wave topology, the pressure distribution, and also the boundary layer (BL) development on the suction side of the blade.

An experimental program was carried out in a transonic wind tunnel in the test sections shown in Figure 2. The flow structure was investigated in the model of a compressor blade passage. The lower and upper profiles were located in a similar configuration as in the reference linear cascade (delivered by the industrial partner—Rolls Royce) in order to keep a similar flow structure as in the reference one. There was a nozzle with a uniform velocity region at its outlet upstream of the blade passage. The Mach number upstream of the blades was supersonic, $M = 1.22$, and the Reynolds

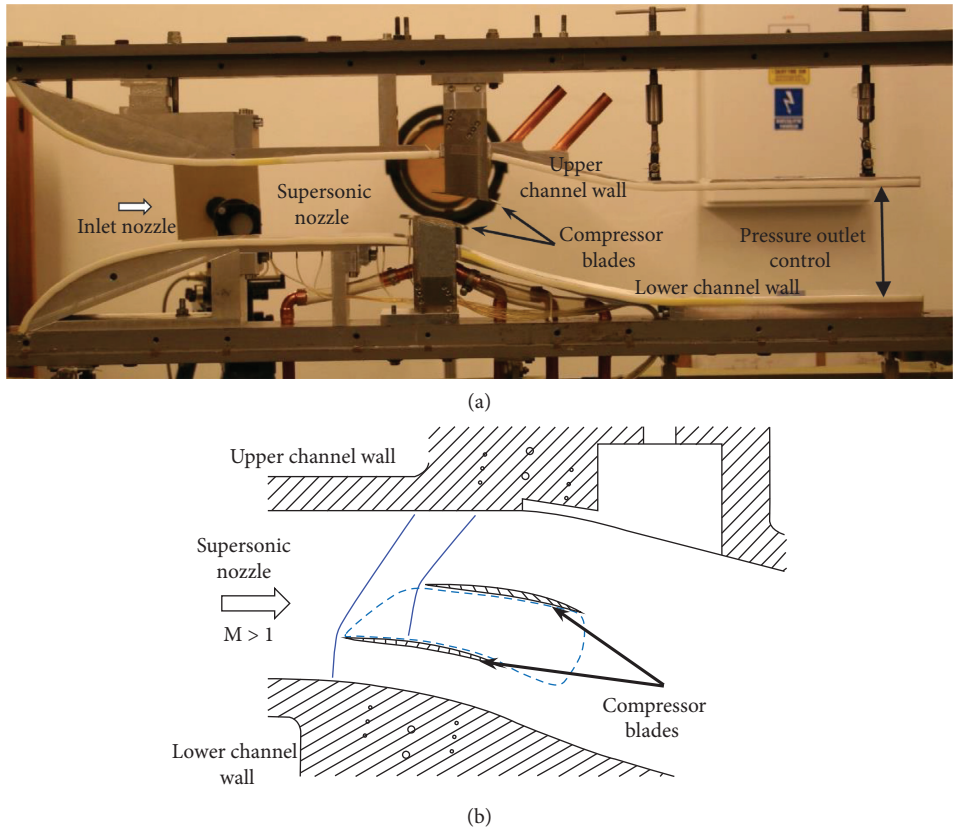

Figure 1: (a) View of the test section in the transonic wind tunnel. (b) Test section layout.

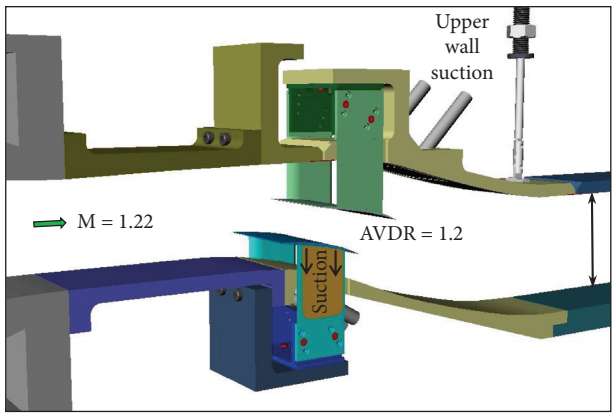

Figure 2: Single-passage compressor cascade model.

number based on the blade chord was 1.4×10^6, which corresponded to the aircraft cruise altitude condition. Both the blade cord c and the blade span were 100 mm long. The blade thickness in the largest cross section was around 3 mm. The interblade channel height-to-chord ratio was 0.6. More details of the compressor cascade model configuration are included in [21]. The turbulence level in the nozzle measured upstream of the passage by the LDA system was 0.8%.

A normal shock wave was generated in the supersonic flow upstream of each blade and interacted with the boundary layer of the neighbouring blade on its suction side (see Figure 1). The flow accelerated the downstream of the blade leading edge up to $M = 1.42$, and the supersonic region was terminated by a normal shock wave. The interaction at such a high Mach number induced a fully unsteady separated flow.

Good mapping of the flow of the compressor channel in the transonic tunnel is a challenge of sorts, because, in reality, such a channel is convergent and there is a pressure increase in the streamwise direction, while the side walls are parallel in the wind tunnel. The parameter that shows whether the flow is well represented is the AVDR (Axial Velocity Density Ratio) of the investigated passage. The appropriate AVDR in the cascade model (Figure 2) is achieved by using a complex suction system. Details of this system can be found in [21]. The AVDR in the single-passage compressor test section used in the experiment was 1.2, as assumed in the design conditions.

The boundary layer thickness measured roughly (roughly because of the problem with seeding in a laminar layer in this location) by the LDA system upstream of the shock at $X/C = 0.3$ was about 0.4 mm. Without transition control, the laminar boundary layer reached the shock wave interaction zone. The location of the main shock wave in the blade passage was at $X/C = 0.48$. It should be kept in mind that the interaction onset starts upstream of the main shock location. Depending on the type of interaction (laminar or turbulent), it occurs more or less upstream of the main shock position. The interaction onset starts at about $X/C = 0.35$ for the laminar type.

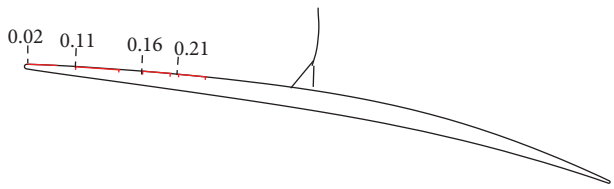

Figure 3: Turbulator strip locations on the blade.

Two types of transition devices (turbulators) were used, namely, microsteps and distributed roughness. Figure 3 shows schematically the locations of all turbulators in relation to the leading edge. The values in this figure show nondimensional distance from the leading edge, i.e., the distance is normalized by the blade chord ($C = 100$ mm). The microsteps were placed in two locations, i.e., at $X/C = 0.02$ and $X/C = 0.16$. The microstep height was the same in both locations being equal to 100 μm. A summary of the microstep configuration in the experiment is given in Table 1. Three locations of the distributed roughness strip were chosen to force the transition, at $X/C = 0.11$, $X/C = 0.16$, and $X/C = 0.21$. The strip width was 5 mm at the locations at $X/C = 0.16$ and 0.21 and 10 mm at $X/C = 0.11$. A different blade model was used to accommodate different roughness positions for each strip location. The investigated cases listed in Table 2 give altogether 9 different flow cases for measurement. The spanwise width of the rough and microstep strips was 100 mm, the same as for the blade. The distributed roughness, from its nature, turbulizes the flow in the boundary layer stronger; hence, its locations are predicted closer to the shock wave position in relation to microsteps.

The distributed roughness was obtained by means of sandpaper strips glued in the prepared groove on the blade. The groove depth was 0.4 mm, and it was oriented in the spanwise direction. The rough strip was stuck on in such a way that the average level of roughness was more or less at the same level as the smooth surface of the blade. Different sorts of sandpapers were used as distributed roughness strips in the experiment, and their average roughness Ra was measured by means of a microscope for the specific sandpaper grit corresponding to the values shown in Table 2, and also, the position of the rough strip in relation to the smooth surface was controlled by means of a microscope [4].

The following measurements were made to investigate some aspects of the boundary layer transition effects on the SWBLI area:

Static pressure distribution along the centre line of the blade

Schlieren visualization of the flow structure and the shock system topology

High-speed Schlieren visualization of normal shock wave oscillations

Oil flow visualization on the blade suction side to display the separation size and structure

Flow velocity distribution across the blade wake by means of LDA (Laser Doppler Anemometry)

Table 1: Step location on the compressor blade.

Strip location (-)	$X/C = 0.02$	$X/C = 0.16$
Strip width (mm)	5	5
Step height (μm)	100	100

Table 2: Roughness strip location and its average height (Ra) on the compressor blade.

Strip location (-)	$X/C = 0.11$	$X/C = 0.16$	$X/C = 0.21$
Strip width (mm)	10	5	5
Roughness height Ra (μm)	8	12	12
	10	16	16
	12	20	20

As has been already mentioned, the paper addresses the flow unsteadiness in a compressor fan passage; hence, the results of the analysis will focus mainly on shock wave oscillations.

3. Results and Discussion

Before we move on to discussing the main results of the experiment on the unsteady effects in the compressor cascade flow, first, it is necessary to present the flow and shock wave pattern in the examined passage. Figure 4 shows the Schlieren flow visualization for a reference laminar interaction. As there is a supersonic flow upstream of the passage, a detached shock wave is created before each blade (profile), denoted as the leading edge shock in the figure. Our area of interest is the flow in the passage; hence, we will focus on the second leading edge shock generated by the upper profile. This shock wave interacts with the lower profile boundary layer, and in consequence, a shock lambda foot appears with some compression waves upstream of it. The main flow features, such as the shocks generated upstream of the leading edge and the shock location on the lower profile, are very similar and correspond to the flow pattern as in the reference compressor cascade [20].

Figures 5 and 6 show selected pictures from oil visualization on the suction side of the blade for the reference case and one of the turbulent interactions, namely, with forced transition by a tripping device. Oil visualization is a simple technique, which, in short, presents the streamline distribution on the investigated surface. For this purpose, a slurry of titanium dioxide in silicone oil is prepared and then distributed on the surface to be tested. During the flow, the slurry is mapping the streamlines, particularly at places with a different skin friction coefficient. First of all, it is shown in Figures 5 and 6 how the separation zone was changed after the application of the transition control method. It is important with respect to the changes of the flow unsteadiness modified by the separation zone structure which influences the pressure distribution in the passage. These figures show a view into the blade suction side through a side wall window. The flow is from left to right.

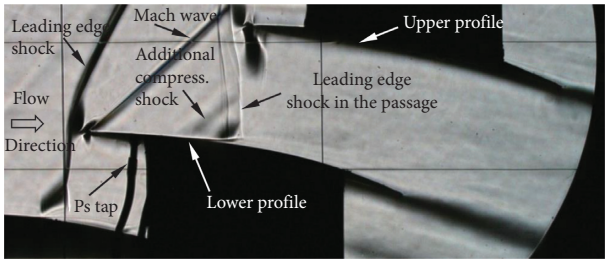

Figure 4: Schlieren flow visualization for reference laminar interaction.

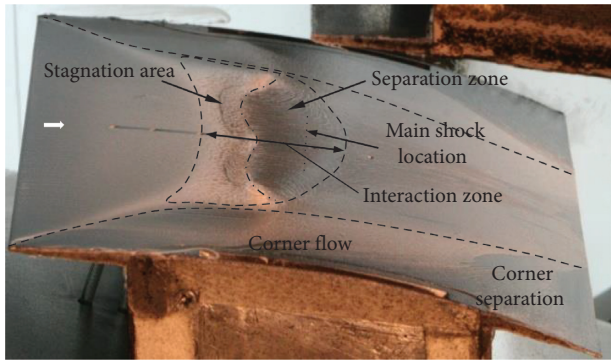

Figure 5: Oil visualization for the reference flow.

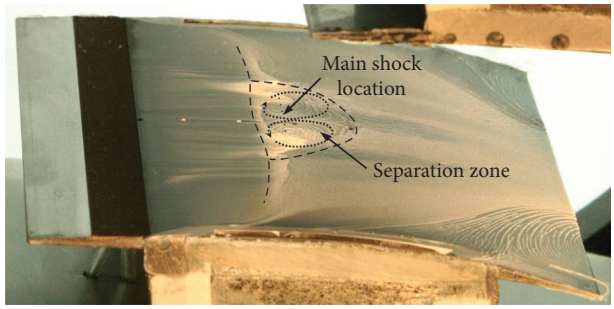

Figure 6: Oil visualization for the flow with roughness at $X/C = 0.11$ and $\mathrm{Ra} = 10\,\mu\mathrm{m}$.

A view of the whole blade for the reference laminar interaction is presented in Figure 5. The laminar interaction means that actually the incoming boundary layer is laminar at the onset of the interaction, and the transition process is induced due to the interaction with the shock wave; finally, a turbulent boundary layer exists downstream of the shock [22]. In this figure, it can be observed that there is an area at the side walls, formed as a result of the interaction between the corner and the main flow. The interaction in the corner starts to develop just downstream of the leading edge, widening considerably at the shock wave-boundary layer interaction area (in the middle of the channel); then, the growth of the corner interaction width slows down. The main shock location is marked by a dotted line drawn transverse to the flow direction. The thicker oil layer upstream of the shock (dashed curve) was created due to the reduced skin friction induced by the shock and means the onset of the interaction. The whole area of interaction (the dashed closed curve) includes two subzones, namely, the stagnation and separation zones. The stagnation zone starts at the location where the additional compression oblique shock (see Figure 4, Schlieren visualization) origins at the blade wall. The separation zone displays a reverse flow area before reaching the dashed curve indicating reattachment. Generally, the size of the laminar interaction on the compressor blade in supersonic conditions is very large and occupies about a quarter of the blade cord.

Oil visualization for the chosen flow case with turbulent interaction (the rough strip position at $X/C = 0.11$) is shown in Figure 6. In this figure, it can be observed that the boundary layer turbulization significantly influences the corner flow, the beginning of the interaction is shifted further downstream, and the oil-thickening layer (interaction onset) starts typically for a turbulent interaction in the vicinity of the λ-foot front shock wave [7]. Moreover, the transition forced by the roughness causes a significant reduction in the separation size in relation to the laminar interaction (see Figures 5 and 6). In the turbulent case, the separation area based on the oil visualization diminishes a magnitude around 60% in relation to the reference flow.

These types of limited separations' zones as in Figures 5 and 6 are strongly three-dimensional. This is not different in these cases either, and axisymmetric large vortices' structures can be seen in the separation area. They have the opposite sense of rotation as indicated by the arrows in Figure 6. On the basis of the literature [14], it can be said that these are two tornado-like eddies, and their size is not exceeding the boundary layer. Such structures have their dynamics, and the frequency related to the rotation of such vortex will translate into shock oscillations in the range of about 100–300 Hz. The effects connected with the compressibility will be characterized by lower dynamics.

3.1. Flow Unsteadiness. The flow unsteadiness in the blade passage was determined by shock oscillation measurements, which, as mentioned, are a derivative of the flow unsteadiness in the separation zone [14]. In general, the shock system was stable and can be considered as a low-pass filter, and the shocks were less stable for lower frequencies. The results were obtained from films based on the Schlieren visualization. The time interval of the analysed films concerns a fully developed shock wave-boundary layer interaction. The films were made using a fast CCD camera and single frames were extracted. One line from each frame only, which crosses the main shock, wave was analysed. The location of the line for the shock oscillation measurements is shown in Figure 7. The distance from the blade wall to the measurement line was about 20 mm. The sampling frequency for all measurements was equal to 2 kHz.

Tables 3 and 4 present the results of the flow unsteady measurements for cases with a microstep and distributed roughness, respectively. The tables show the amplitude values A and the average RMS oscillations of the main shock for different flow cases measured. The amplitude magnitude

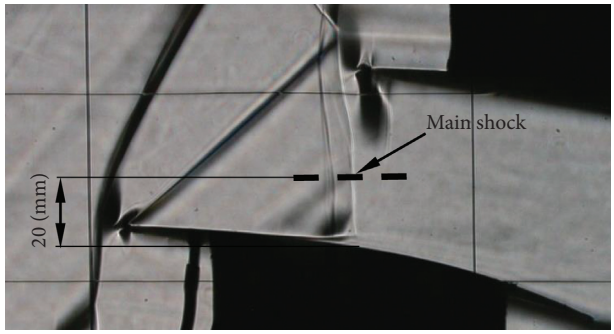

Figure 7: Measurement locations by the fast CCD camera.

Table 3: RMS of average shock oscillations and shock amplitude for flow cases with the microstep.

Flow case	A (mm)	RMS (mm)
Ref-laminar	4.37	1.21
$X/C = 0.02$	4.73	1.22
$X/C = 0.16$	3.64	1.16

Table 4: RMS of average shock oscillations and shock amplitude for flow cases with roughness.

Flow case	A (mm)	RMS (mm)
Ref-laminar	4.37	1.21
$X/C = 0.11$, Ra = 8	4.84	1.33
$X/C = 0.11$, Ra = 10	3.96	1.04
$X/C = 0.11$, Ra = 12	4.84	1.07
$X/C = 0.16$, Ra = 12	4.71	1.54
$X/C = 0.16$, Ra = 16	5.04	1.52
$X/C = 0.16$, Ra = 20	4.45	1.20
$X/C = 0.21$, Ra = 12	5.48	1.57
$X/C = 0.21$, Ra = 16	6.28	1.85
$X/C = 0.21$, Ra = 20	4.63	1.24

displays the shock movement in the passage, and RMS represents the effective value of its oscillations.

From the application point of view, it is not only losses but also the unstable blade loading resulting from flow unsteadiness that are important. It should be kept in mind that the flow unsteadiness in the blade passage will be affected not only by the type of the boundary layer (laminar and turbulent) but also by the parameters of the turbulent layer, such as its thickness and shape factor. Early turbulization of the layer before the shock (a relatively large distance to the shock) will cause an excessive increase in its thickness, and the shape parameter will increase, and thus, the ability to withstand the adverse pressure gradient which is induced by the presence of the shock wave in the channel will decrease. This, in turn, may cause an increase in the separation area and an increase in the flow unsteadiness. Therefore, it is very important not to exaggerate with the development of the turbulent layer, i.e., it should take place in the right place in order not to get the opposite effect and not to cause an increase in the nonstationary effects.

The flow case with a microstep for which the unsteadiness was reduced in relation to the reference flow is $X/C = 0.16$. Both the shock amplitude and RMS for this flow case decrease, the amplitude of approx. 15% and RMS of approx. 5%. The flow case with a microstep at the leading edge ($X/C = 0.02$) inscribes in the mechanism described above and the unsteadiness increases as a result.

As far as flow unsteadiness with application of roughness is considered, the general tendency in relation to the reference flow is the growth of both the shock amplitude and the RMS for almost all flow cases except for one. A reduction in the average shock oscillations as well as the shock amplitude were received for one flow case only with roughness $\mathrm{Ra} = 10\,\mu\mathrm{m}$ located at $X/C = 0.11$. However, a decrease in RMS was achieved as well for the same location, but for $\mathrm{Ra} = 12\,\mu\mathrm{m}$. Moreover, in many cases, the growth of shock oscillations is rather moderate being approx. 10%. Generally, for the cases with roughness, the flow unsteadiness is the lowest for the cases where the distance between the rough strip location and the shock position is the highest. Unlike with the microstep, the roughness height is about one order smaller, but it generates a more uniform distribution of the turbulence, and perhaps, more distance is needed for a fully developed turbulent boundary layer to form. Therefore, a proper boundary layer turbulization is favourable for the decreasing flow unsteadiness, and the boundary layer in flow cases with roughness closer to the shock location is still in a process of transition.

The above results show global properties of unsteadiness in the investigated blade passage such as the amplitude and RMS of shock oscillations; however, the spectral analysis is also very important, i.e., what the signal distribution looks like in the frequency domain? For this purpose, the FFT transformation of signals was performed for selected flow cases. The information about the shock wave motion in the form of a signal power spectrum (PS) of shock oscillations is shown in Figures 8–13. The reference case is shown in Figure 8. Based on this figure, it can be noticed that some predominant frequencies can be distinguished in the case of the laminar interaction; there are some peaks around 5 Hz in the range of low frequencies up to 10 Hz and a peak of approx. 50 Hz that can be distinguished in the next interval in the range of 10–100 Hz. The power of the shock amplitude decreases significantly approximately above 500 Hz.

Figures 9 and 10 show the influence of the microstep application on the flow unsteadiness in two different locations. Comparing Figures 9 and 10 with the reference case (see Figure 8), it can be observed that the shock oscillations decrease first in a range of up to 10 Hz. It would indicate a reduction in the unsteadiness linked with the separation region, which often manifests itself in a range of low frequencies, and their source is related to successive contractions and expansions of the separated bubble. Hence, the reduction of separation size can also have influences on diminution of the flow unsteadiness; smaller volume pulsates with lower amplitude. In the case of a microstep located at $X/C = 0.16$ (see Figure 10), it can be observed that the flow was calmed down over the entire range of frequency. Slightly different results were obtained in the case of a microstep

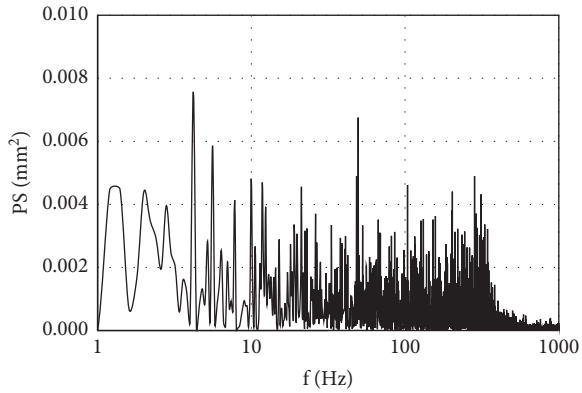

Figure 8: Power spectrum of shock oscillations for laminar interaction.

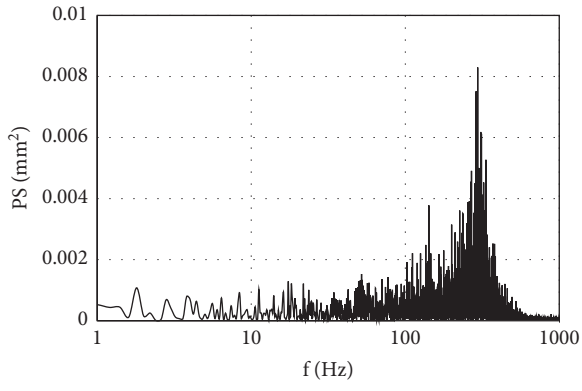

Figure 9: Power spectrum of shock oscillations for microstep at $X/C = 0.02$.

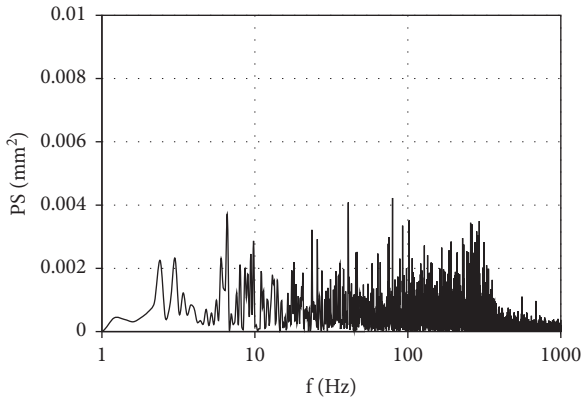

Figure 10: Power spectrum of shock oscillations for microstep at $X/C = 0.16$.

located at the leading edge, see Figure 9. In this case, the oscillations of the shock wave are very low for frequencies up to 100 Hz. As the frequency increases above 100 Hz, the oscillations tend to increase leading to a characteristic frequency of approx. 300 Hz, at which the power spectrum amplitude was approximately two times higher in relation to

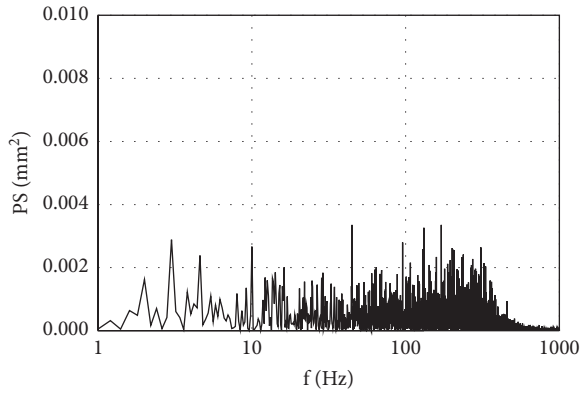

Figure 11: Power spectrum of shock oscillations for roughness at $X/C = 0.11$ and $\mathrm{Ra} = 10\,\mu$m.

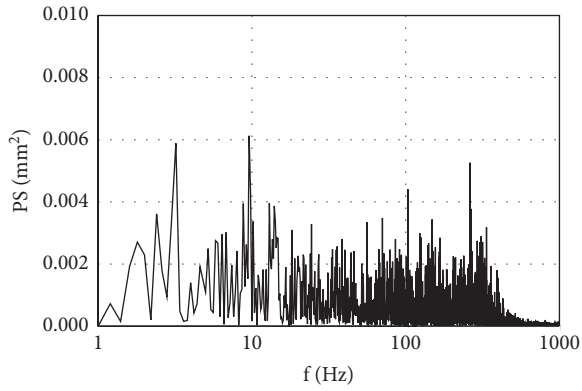

Figure 12: Power spectrum of shock oscillations for roughness at $X/C = 0.16$ and $\mathrm{Ra} = 20\,\mu$m.

the reference flow. Such frequency distribution may indicate some influence of the shock system near the leading edge on the flow structure generated behind the microstep. This disturbance is likely to propagate further downstream and increase the intensity of the eddies in the separation region induced by the main shock in the blade passage. Generally, the flow case with a microstep located at $X/C = 0.16$ shows that the transition induced in the appropriate location can reduce the shock wave oscillation, both RMS and the amplitude. The RMS of the shock oscillations is about 1% of the blade cord.

Figures 11–13 show the results of shock wave oscillation measurements for flow cases with distributed roughness. There were chosen cases one for every roughness locations which give the lowest oscillations in terms of RMS. It can be seen that the frequency distribution of shock oscillations for these cases is very similar i.e., there is no clear dominant frequency which can be distinguished. In Figure 11, one can observe a clear calming down of the flow for the roughness position at $X/C = 0.11$ ($\mathrm{Ra} = 10\,\mu$m), practically over the entire frequency range, which is confirmed by a decrease in the effective value of the shock oscillations and its amplitude in Table 4. For the flow case with roughness strip at $X/C = 0.16$, see Figure 12, only a slight decrease in the

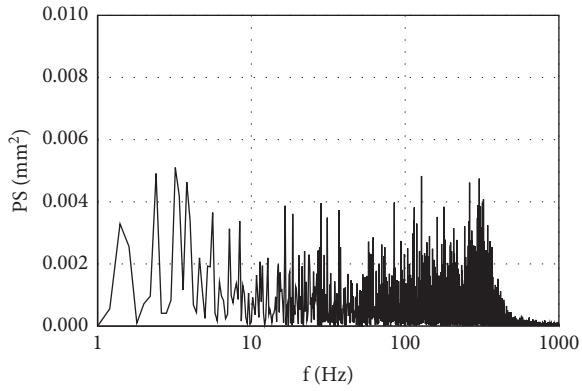

Figure 13: Power spectrum of shock oscillations for roughness at $X/C = 0.21$ and $\mathrm{Ra} = 20\,\mu\mathrm{m}$.

oscillations' amplitude in the low frequency ranges up to about 10 and 100 Hz can be observed. In the case of the roughness even closer to the shock wave at $X/C = 0.21$, see Figure 13, in comparison to the previous flow case (see Figure 12, $X/C = 0.16$), it obtained a slight decrease in the oscillation amplitude in the low-frequency range to about 10 Hz. As has been already mentioned above, the high peaks at low frequencies for the reference flow are connected with the unsteadiness in the separation area, the size of which is significant, and therefore, the low frequencies are dominating. In the case when the separation size is reduced, the low frequencies stop to play an important role and higher frequencies start to dominate, as shown in Figure 11.

4. Conclusions

The obtained results from the above-presented experimental investigations show that the induction of a properly configured transition, upstream of the shock, has positive influence on the shock wave-boundary layer interaction region in the context of the flow unsteadiness in a compressor cascade blade passage. A reduction in the shock wave unsteadiness was observed in the flow in the case of some turbulent interactions. It can be also observed that application of improper control method produces negative impact on the flow characteristics.

Two methods of transition control were tested in the described above research, i.e., microsteps and distributed roughness located upstream of the shock wave-boundary layer interaction. For each of these methods, it was possible to show the positive influence of their application on the flow unsteadiness in the compressor blade passage. Conclusions on the location of the flow transition control vary according to the type of the method used.

In the case of microstep applications, a better location is closer to the shock wave. In the examined case, it was $X/C = 0.16$, and in this location, the flow was calmed down over the entire frequency range, without amplifying large eddy structures inside the separation area.

In the case of using distributed roughness to control the boundary layer transition, conclusions about the location are different to some extent. For this transition control method, a better location is a longer distance upstream of the shock wave, closer to the leading edge, approximately at $X/C = 0.11$. With regard to roughness size, small values are preferred for the best location, approx. $\mathrm{Ra} = 10\,\mu\mathrm{m}$. In the case of two locations closer to the shock wave, in terms of the flow stabilisation, higher roughness values are better; however, for these values, what is known from other investigations, an increase in the flow losses in the blade wake is also achieved. Small values of roughness closer to the leading edge are the reason why the boundary layer has a long distance to develop a full turbulent profile without not too much growth of its thickness, and in consequence, a flow stabilizing in the whole blade passage.

From both the applied transition control methods, roughness seems to be more promising. In this case, due to its size (a few microns), it interferes with the flow less, and the results in terms of reduction of unsteadiness (RMS) are more favourable compared to the microstep.

To summarize the presented investigations on the flow unsteadiness in a compressor blade passage with the shock boundary layer interaction, it can be said that it is a very complex issue because it shows that a full turbulent profile of the boundary layer with modest growth of its thickness is needed to achieve the desired effects. More detailed research is needed to determine the condition of the boundary layer upstream of the shock, which would show why cases from roughness application closer to the interaction area give unsatisfactory results in terms of flow instability in the examined blade passage.

Data Availability

The datasets used in the present study are available from the corresponding author upon reasonable request.

Conflicts of Interest

The authors declare that they have no conflicts of interest.

Acknowledgments

The research leading to these results received funding from the European Union Seventh Framework Programme (FP7/2007–2013) under grant agreement (no. 265455) (TFAST [23]), which studied the effects of the boundary layer transition on the shock wave-boundary layer interaction.

References

[1] R. Messing and M. J. Kloker, "Investigation of suction for laminar flow control of three-dimensional boundary layers," *Journal of Fluid Mechanics*, vol. 658, pp. 117–147, 2010.

[2] H. V. Moradi and J. M. Floryan, "Laminar flow in grooved pipes," *AIAA Journal*, vol. 55, no. 5, pp. 1749–1752, 2017.

[3] N. Beck, T. Landa, A. Seitz, L. Boermans, Y. Liu, and R. Radespiel, "Drag reduction by laminar flow control," *Energies*, vol. 11, no. 1, p. 252, 2018.

[4] R. Szwaba, P. Kaczynski, and P. Doerffer, "Roughness effect on shock wave boundary layer interaction area in compressor fan blades passage," *Aerospace Science and Technology*, vol. 85, pp. 171–179, 2019.

[5] P. Flaszynski, P. Doerffer, R. Szwaba, M. Piotrowicz, and P. Kaczynski, "Laminar-turbulent transition tripped by step on transonic compressor profile," *Journal of Thermal Science*, vol. 27, no. 1, pp. 1–7, 2018.

[6] P. Flaszynski and R. Szwaba, "Experimental and numerical analysis of a streamwise vortex generator for subsonic flow," *Chemical and Process Engineering-Inzynieria Chemiczna I Procesowa*, vol. 27, no. 3, pp. 985–997, 2006.

[7] R. Szwaba, "Comparison of the influence of different air-jet vortex generators on the separation region," *Aerospace Science and Technology*, vol. 15, no. 1, pp. 45–52, 2011.

[8] R. Szwaba, "Influence of air-jet vortex generator diameter on separation region," *Journal of Thermal Science*, vol. 22, no. 4, pp. 294–303, 2013.

[9] H. Kobayashi, "Effects of shock waves on aerodynamic instability of annular cascade oscillation in a transonic flow," *Journal of Turbomachinery*, vol. 111, no. 3, pp. 222–230, 1989.

[10] T. J. Carter, "Common failures in gas turbine blades," *Engineering Failure Analysis*, vol. 12, no. 2, pp. 237–247, 2005.

[11] J. S. Rao and A. Saldanha, "Turbomachine blade damping," *Journal of Sound and Vibration*, vol. 262, no. 3, pp. 731–738, 2003.

[12] M. Swoboda and W. Nitsche, "Shock boundary-layer interaction on transonic airfoils for laminar and turbulent flow," *Journal of Aircraft*, vol. 33, no. 1, pp. 100–108, 1996.

[13] B. Becker, M. Reyer, and M. Swoboda, "Steady and unsteady numerical investigation of transitional shock-boundary-layer-interactions on a fan blade," *German Aerospace Congress*, vol. 11, no. 7-8, 2006.

[14] J.-P. Dussauge, P. Dupont, and J.-F. Debiève, "Unsteadiness in shock wave boundary layer interactions with separation," *Aerospace Science and Technology*, vol. 10, no. 2, pp. 85–91, 2006.

[15] J. P. Dussauge, S. Piponniau, J. F. Debiève, and P. Dupont, "A simple model for low frequency unsteadiness in shock induced separation," *Journal of Fluid Mechanics*, vol. 629, pp. 87–108, 2009.

[16] N. Titchener and H. Babinsky, "A review of the use of vortex generators for mitigating shock-induced separation," *Shock Waves*, vol. 25, no. 5, pp. 473–494, 2015.

[17] H. Babinsky and G. R. Inger, "Effect of surface roughness on unseparated shock-wave/turbulent boundary-layer interactions," *AIAA Journal*, vol. 40, no. 8, pp. 1567–1573, 2002.

[18] R. H. M. Giepman, R. Louman, F. F. J. Schrijer, and B. W. Van Oudheusden, "Experimental study into the effects of forced transition on a shock-wave/boundary-layer interaction," *AIAA Journal*, vol. 54, no. 4, pp. 1313–1325, 2016.

[19] N. Fomin, E. Lavinskaya, P. Doerffer, J.-A. Szumski, R. Szwaba, and J. Telega, "Quantitative diagnostics of shock wave—boundary layer interaction by digital speckle photography," *Shock Waves*, vol. 1, pp. 457–462, 2009.

[20] M. Piotrowicz and P. Flaszynski, "Numerical investigations of shock wave interaction with laminar boundary layer on compressor profile," *Journal of Physics, Conference Series*, vol. 760, no. 1, Article ID 012023, 2016.

[21] P. Flaszynski, P. Doerffer, R. Szwaba, P. Kaczynski, and M. Piotrowicz, "Shock wave boundary layer interaction on suction side of compressor profile in single passage test section," *Journal of Thermal Science*, vol. 24, no. 6, pp. 510–515, 2015.

[22] H. Babinsky and J. K. Harvey, "Shock waveoundaryayer interactions," *Aerospace Series*, Cambridge University Press, Eds., Cambridge, UK, 2011.

[23] P. Doerffer, H. Babinsky, A. Petersen et al., "Transition Location Effect on Shock Wave Boundary Layer Interaction," http://www.tfast.eu, 2020.